A METHOD TO CHARACTERIZE BIOLOGICAL DEGRADATION OF MASS TIMBER CONNECTIONS[1]

Arijit Sinha†*
Associate Professor
E-mail: arijit.sinha@oregonstate.edu

Kenneth E. Udele
Graduate Assistant
E-mail: kenneth.udele@oregonstate.edu

Jed Cappellazzi
Sr. Faculty Research Assistant
Department of Wood Science and Engineering
Oregon State University
119 Richardson Hall
Corvallis, OR 97331
E-mail: jed.cappellazzi@oregonstate.edu

Jeffrey J. Morrell†
Director
National Centre for Timber Durability and Design Life
University of the Sunshine Coast
41 Boggo Road, Ecosciences Precinct
Dutton Park, Queensland 4102, Australia
E-mail: jmorrell@usc.edu.au

(Received June 2020)

Abstract. Biological durability issues in cross-laminated timber (CLT) have been majorly ignored in North America because of the European origin of the material and careful construction practices in Europe. However, the risks of fungal and insect attacks are increased by the North American climatic conditions and lack of job-site measures to keep the material dry. The methods to evaluate durability in solid timber are inadequate for use in mass timber (MT) for a number of reasons, such as moisture variation and size being critical issues. This study therefore proposes a method, which is suitable to evaluate the strength of MT assemblies that are exposed to fungal degradation. The objective of the study was to explore a controlled method for assessing the effects of wetting and subsequent fungal attack on the behavior of CLT connections. Two different methods were used to create fungal attack on CLT assemblies. Although they were both successful, one was cumbersome, left room for many errors, and was not as efficient as the other. In addition, a standardized method to evaluate and characterize key performance metric for the connections is presented.

Keywords: Biological durability, fungi, CLT connections, connection strength.

INTRODUCTION

Mass timber (MT) is an increasingly popular group of building materials. Introduction of cross-laminated timber (CLT) and mass plywood panels has enabled designers to pursue timber-based design solutions for mid- to high-rise buildings (Mallo and Espinoza 2014; Kremer and Symmons 2015; Brandner et al 2016; Fast et al 2016). The popularity of MT was highlighted when the International Code Council ratified recommendations for increasing the limit for MT to 18

* Corresponding author
† SWST member

stories (up to 9 if MT is exposed). The rapid adoption of this technology in North America and acceptance in the building codes have been driven by a robust body of research. Although there has been a tremendous effort to characterize and modify MT for the North American market (Kippel et al 2014; Kramer et al 2014, 2016; Hasburgh et al 2016a, 2016b; Pei et al 2016, 2019; Ganey et al 2017; Mahdavifar et al 2017; Tugce et al 2017; Barber 2018; Barbosa et al 2018; Bolvardi et al 2018; Schmidt and Blass 2018; Tannert et al 2018; Blomgren et al 2019; van de Lindt et al 2019; Fitzgerald et al 2020; Miyamoto et al 2020; Morrell et al 2020; Soti et al 2020), the risk of moisture intrusion and subsequent development of fungal and insect attack has largely been ignored (Cappellazzi et al 2020). Part of this complacency lies with the lower decay risks present in Central Europe and the absence of termites where MT first emerged as a viable building product coupled with building practices that better control moisture intrusion during construction.

However, several recent reviews have highlighted the potential risks of using MT elements in more decay-prone conditions (Wang et al 2018; Cappellazzi et al 2020), other studies have illustrated the risks of water intrusion in MT elements during construction (Glass et al 2013; Morrell et al 2018; Schmidt et al 2019), and Wang et al (2018) highlighted the contribution of plumbing leaks and overflows, pipe condensation, and occupant-caused wetting.

Although many organisms can invade wet wood, fungal decay is the most common cause of building damage closely followed by termites in areas where these insects are prevalent (Mankowski and Morrell 2000). The most important fungi are the basidiomycetes, which include nearly all of the important building decay organisms. Prolonged wetting leads to colonization of decay fungi (e.g., brown rot or white rot), which can survive within for years and eventually degrade the wood when conditions are suitable for growth (Kent et al 2007; Wang et al 2018).

Assessing the effects of moisture intrusion and biological degradation on MT properties will require cross-disciplinary collaboration. Cappellazzi et al (2020) emphasized a need for a broader effort pursued jointly by multiple stakeholders. One critical limitation is the lack of standardized protocols for evaluating MT durability.

Although there are a variety of methods available to evaluate timber durability, most are not appropriate for MT. Laboratory tests typically use very small pieces of wood, making it difficult to create test samples that encompass the features of an MT panel. Field trials tend to expose timber to outdoor weathering to accelerate decay. However, MT is not likely to be fully exposed to wetting. Instead, the process will likely move from wetting at some point during construction or in service followed by fungal attack. Field trials also tend to use smaller timber samples. All of the current standard decay test methods tend to expose small timber samples to wetting regimes that would be far in excess of what might occur in MT. In addition, the sample dimensions are too small to incorporate the physical behavior characteristic that might occur in a full-scale member.

The objective of this study was to explore a controlled method for assessing the effects of wetting and subsequent fungal attack on the behavior of a CLT connection system. There is a lack of well-defined guidelines on parameters that are more important for assessment of connection systems. The assessment procedure is based on the quantification of performance using cyclic tests before and after the controlled wetting and fungal attack regimen, from which the parameter degradation rate is used as an indicator for classifying the durability of MT connections.

METHODS FOR INVESTIGATION OF CLT

Evaluation of Decay Susceptibility

The test configuration was designed to 1) use representative material dimensions, 2) create realistic moisture intrusion, 3) incorporate effects of moisture on connection properties, and 4) produce a representative risk of fungal degradation. The intent of the degradation experiment was to subject properly scaled CLT connections to a "worst case scenario" of biodeterioration, not

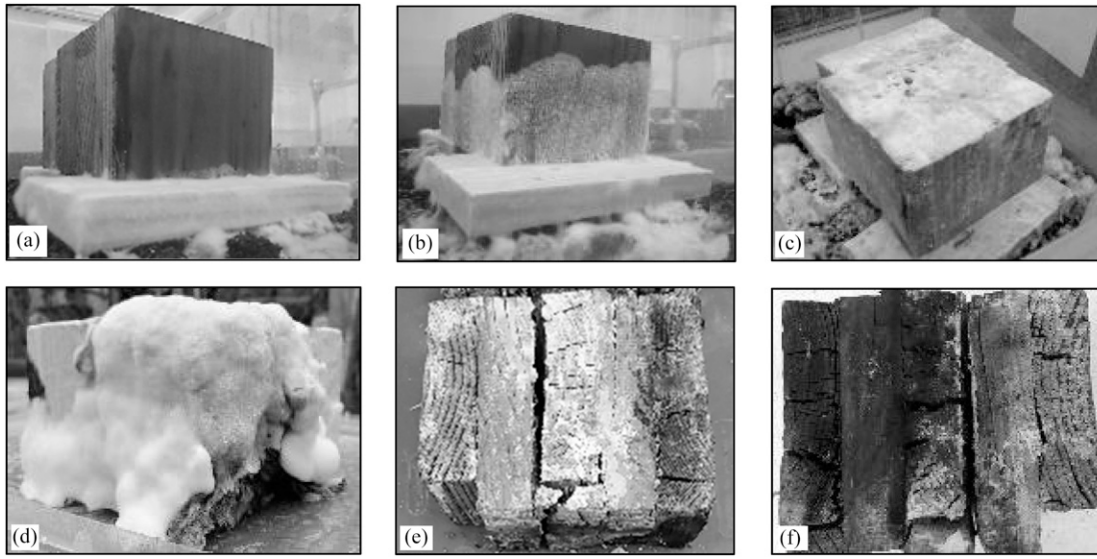

Figure 1. Progression of fungal growth over Douglas-fir cross-laminated timber (CLT) samples exposed to *Rhodonia placenta* for (a) 3 d, (b) 20 d, (c) 61 d, and (d) 264 d after inoculation as well as examples of the bottom of the same sample in direct contact with the test fungus before (e) and after (f) oven drying.

necessarily to mimic natural exposure in a building (Fig 1). This section describes two distinct methods to successfully inoculate the specimen with decay fungi.

The two different methods evaluated two specimen sizes. The first used larger samples designed to evaluate the effects of wetting and fungal attack on connector capacity. The test proved cumbersome in terms of sample dimensions and logistics. Therefore, a second procedure was examined involving decay on smaller specimens that were designed to be easy to soak, sterilize, and expose to the test fungi.

The connection assemblies in the first method were three-ply Douglas-fir (*Pseudotsuga menziesii* var. *menziesii*) ANSI PRG320 V1 CLT (104-mm-thick, 200-mm-wide, and 305-mm-long) panels. Two pieces of CLT were joined using a galvanized steel (12-gauge ASTM A653 Grade 33, 227.5 MPa yield strength) L-bracket connection (Fig 2). Two 15.9-mm-diameter A307 Grade A (ASTM 2014b) hex bolts and eight 8-d common smooth shank nails were used to complete the connection. The connection was assembled with the strong axis of the wall piece oriented vertically, as is common in most CLT shear wall systems. In accordance with the National Design Specification for wood construction, the bolt holes drilled into the bottom piece were oversized by 1.60 mm (1/16th in.) in relation to the bolt diameter (AWC 2018). Three assemblies were prepared: one was a no fungus and no exposure control, the second assembly was inoculated with *Gloeophyllum trabeum* (Pers ex Fr.) Murr. (Isolate # Mad 617), and the third

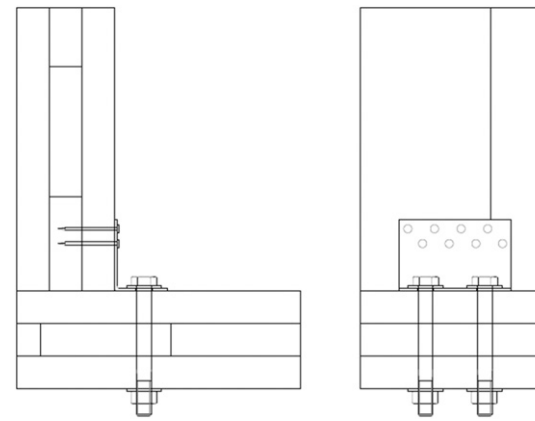

Figure 2. Schematic of the connection test specimen.

was inoculated with *Rhodonia placenta* (Fr) Niemela, Larss, and Schagel (Isolate # Mad 698).

The test samples were first conditioned to constant weight in a standard room maintained at 20°C and 65% RH before being weighed and then immersed in water for approximately 5 wk at room temperature until they reached an average MC of 40%. The samples needed to be saturated to aid fungal growth. Four small holes (3.2 mm) were drilled into the wide face near the junction of the two pieces and marked for future fungal inoculation. The next step was to sterilize the samples. For that, specimens were wrapped in sturdy autoclavable bags (1.5 mm thick), one from each end, filled with 100 mL of deionized water, and loosely tied in the middle before being autoclaved at 121°C for 60 min (Fig 3). After cooling, the bags were placed in individual aluminum trays to minimize the risk of damage as bags were moved. The test fungi were introduced by injecting 10 mL of liquid culture of the respective fungus into the four predrilled holes until it overflowed on the wood surface. The bags were sealed and incubated in a standard room maintained at 20°C and 65% RH for 425 d (14 mo). At the end of the incubation period, the samples were removed from the standard room, scraped clean of adhering mycelium, and reconditioned to constant weight at 20°C and 65% RH before being weighed. The difference between initial and final conditioned weight was used to calculate fungus-associated weight loss.

Figure 3. Example of a Douglas-fir connector assembly inoculated with *Gloeophyllum trabeum* showing minimal fungal growth on the outside of the wood.

The first method eventually resulted in fungal degradation, the process was time- and labor-intensive, and the bags were prone to damage that would allow other organisms to contaminate the wood. Thus, a second method was used to degrade the connection samples. In the second method, ten 104-mm-thick three-ply CLT specimens from the same source were cut into samples with volumes of 1785, 2888, or 3600 cm^3. Three samples were southern pine, and the remainder was Douglas-fir. The samples were dried at 50°C for 5 d before being weighed. The samples were immersed in distilled water, and a vacuum (81.3 kPa) was drawn over the water for 30 min; the vacuum was released, and the samples were left in the water for 2 h to raise the MC above 30%. The samples were then autoclaved at 121°C for 60 min.

The decay chambers were 76-L polypropylene gasket boxes (61.0 cm × 45.7 cm × 38.7 cm) that were sterilized in a laminar flow hood using a combination of 10% bleach and 70% ethanol. Boxes were tested with and without 60-mm-diameter vent holes covered with Tyvek™ to allow airflow but exclude fungal propagules. A sterile mixture of 80% vermiculite and 20% potting soil (sandy loam soil, composted dairy/horse manure, fir bark, and Gardner and Bloom Soil Building Conditioner) was saturated to field capacity, and a 50-mm-thick layer was added to the bottom of each chamber to ensure that the blocks remained at moisture levels suitable for fungal growth. A sterile 25-mm-thick by 140-mm × 300-mm-long southern pine sapwood (*Pinus* sp.) wafer was placed on the vermiculite/soil layer to provide wood for the test fungus to grow and to separate the test members form the mixture to avoid excessive wetting that might inhibit fungal attack.

Some chambers were inoculated by placing 10-mm-diameter agar discs cut for the edges of actively growing culture of the test fungus on the edges of the southern pine feeder strips and incubating the chamber until the fungus had

covered the wood. Alternatively, the test fungi were grown on sterile wheat seed grain, and 0.25 L of the fungal colonized seed was evenly distributed over the vermiculite/soil surface. The sterile test pieces were then placed on the feeder strip surface, and the chambers were incubated at 20-22°C for 180-264 d. At the end of the incubate period, the samples were removed, scraped clean of any adhering mycelium of vermiculite/soil, and weighed before being dried to constant weight at 50°C. The blocks were then weighed again. Differences between initial conditioned weight and oven-dry weight were used to calculate the final MC, whereas the differences between initial and final conditioned weight were used to calculate fungus-associated mass loss. Because this was a preliminary trial, test conditions were only evaluated on one or two specimens per variable. Table 1 summarizes the various combination used in this method.

Strength Testing Methods

The connections after exposure to degrading fungi were tested on a 178 kN hydraulic universal testing machine (UTM) in a displacement-controlled cyclic loading protocol. Because the UTM and actuator were set up for vertical load application, the specimens were rotated in the test setup to align the lateral direction with the loading axis of the actuator. The test setup is shown in Fig 4. The bottom piece was held in place using a steel bar on top fastened to the testing table with 17-mm-diameter threaded rods. The loading fixture was custom-made for a series of similar testing and is described in greater detail in Mahdavifar et al (2019) and Mahr et al (2020). The test setup is described in detail in Mahr et al (2020) where the reader is directed for design of the custom fixture. For future research, the design of the custom fixture will however change as per the requirements of accessible UTM. Important things to consider in design of the test setup are that the rotation and translation of the floor plate should be restricted.

For cyclic testing, the actuator head needed to clamp both sides of the specimen wall piece to transmit force in both directions. This was accomplished by using two pieces of steel tubing on the opposite wall side connected to the actuator head with 9.5-mm (3/8 in.) threaded rods (Fig 4). To simulate in situ shear wall conditions for this connection, the rotations of the wall piece were not controlled, leaving the bracket connection itself to resist these rotations.

The cyclic loading was performed according to an abbreviated basic loading history CUREE protocol, developed by Krawinkler et al (2001), with two additional primary cycles beyond the reference deformation (Δ) of 1.5Δ and 2.0Δ, respectively (Fig 5). These additional primary cycles were used to ensure specimen failure. The CUREE reference deformation of 12.7 mm was determined by Mahr et al (2020) according to methods identified in Krawinkler et al (2001) by performing monotonic tests. The loading rate used was 7.2 s per/cycle for 35 cycles, yielding a total loading protocol duration of 4 min and 12 s. The maximum displacement rate was 11.4 mm/s in the final primary cycle. Data collected included actuator load and actuator head displacement,

Table 1. Mass losses of Douglas-fir and southern pine cross-laminated timber samples exposed to white and brown rot fungi for 180-260 d under various decay regimes.

Fungus	Wood species	Wood volume (cm^3)	Vents	Inoculum	Exposure time (d)	Final MC (%)	Mass loss (%)
T. versicolor	Douglas-fir	1785	No	Grain	180	125.7	25.4
R. placenta						86.3	37.6
G. trabeum						70.1	14.9
R. placenta	Douglas-fir ($n = 2$)	1785	Yes	Pine feeder	260	88.1	52.7
		2888				70.8	30.8
T. versicolor	Douglas-fir	3600	No		260	64.6	3.4
P. gigantea	Southern pine ($n = 2$)	1785	No		180	61.3	14.7
G. trabeum		1785	Yes		260	46.7	46.3

Figure 4. Test setup.

which was used as the measure for wall piece deflection relative to the bottom piece.

Parameters Evaluated

The primary cyclic force–displacement data from the testing generated hysteresis curves for each specimen (Fig 6[a]). The backbone curve of the hysteresis curves was developed for each specimen by plotting the maximum first force recorded at each displacement from the hysteresis data, effectively only plotting force from the primary cycles of the CUREE displacement protocol. The backbone curves (Fig 6[a], bold line) were then used to define parameters and/or equations that approximate the force–displacement relationship using a trilinear model as outlined in ASCE 41-17 (Fig 6[b]).

ASCE 41-17 is a guide for engineers to evaluate seismic performance of existing buildings. For MT, which is a material not covered in ASCE 41-17, the guide outlines an alternative method for determining modeling parameters using physical

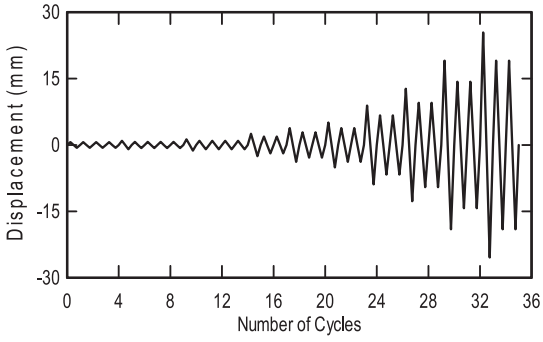

Figure 5. CUREE loading protocol.

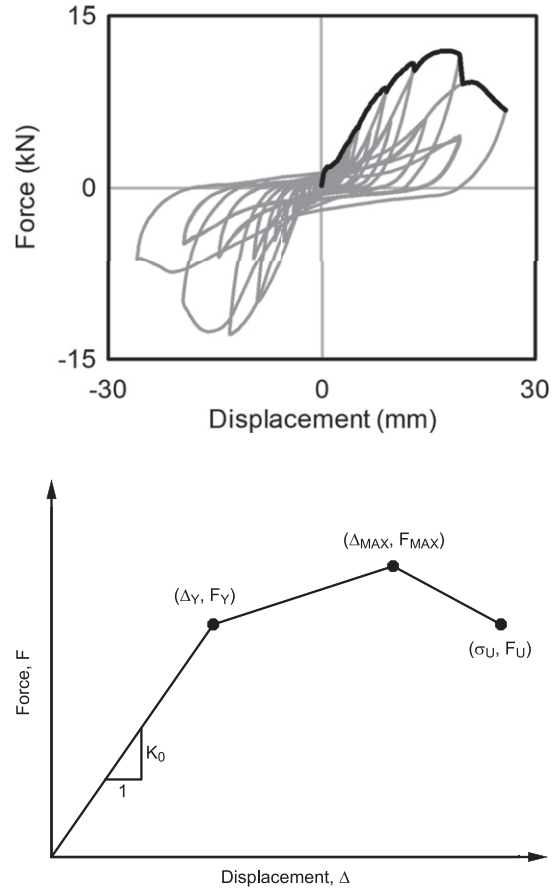

Figure 6. ASCE 41-17 trilinear idealization process.

tests. The curve type that is appropriate for this kind of research is the Type 2 curve as outlined in ASCE 41-17. The Type 2 curve is a composite curve of three linear segments: elastic, post-yield plastic, and post-peak plastic. ASCE 41-17 does not specify a procedure for determining where each of these segments begin and end, leaving it to the discretion of the user. For our purposes, we attempt to define a protocol that has given consistent results over the last few years. The parameters are listed in Table 2 along with their description and protocol used to calculate them. The first line or the initial elastic segment ends at the yield point and has a slope, K_0. The yield point at the end of the elastic segment is defined by the yield strength, F_Y, and yield displacement, Δ_Y. The yield strength was determined using the 5% offset method outlined in ASTM D 5764 (2018). The 5% offset method defines the yield strength as the point at which the backbone curve is intersected by a line with a slope equal to the initial stiffness (K_0) and which is offset to a displacement of 5% of the fastener's root diameter. The initial stiffness (K_0) was determined by performing a regression analysis on a representative linear portion in the elastic region of the backbone curve generally between 0.1 and 0.4 of F_{max}. The next line on the composite curve is the post-yield plastic segment beginning at the yield point and ending at the peak of the backbone curve. The parameters associated with the peak are peak strength, F_{max}, and corresponding displacement, Δ_{max}. The load–deflection coordinate for the peak was taken directly from the backbone curve. The final line of the composite curve is the post-peak plastic segment beginning at the peak and ending at the failure point defined by the failure load, F_U, and ultimate displacement, Δ_U. The failure load and ultimate displacement were taken from the last point on the backbone curve with a load greater than or equal to 80% of the peak load. The ASCE 41-17 idealization process is shown in Fig 6.

PRELIMINARY RESULTS AND DISCUSSION

Physical Changes

At the end of the 425-d period of exposure, the samples showed varying changes in physical properties. These included general physical alterations such as colored stains and patches, exfoliation, and pitting stated by Gaylarde et al (2003). There were differences in the physical changes which were observed in the two different fungi species. Whereas brown patches were noticed on the surface of the assembly with *G. trabeum*, the assembly infested by *R. placenta* showed white patches all over. Figure 7 shows the assembly at different stages of exposure and testing. The blocks also showed a variation in the weight changes over the period of exposure as reported in Table 3. The sample exposed to *G. trabeum* weighed 8.52 kg at testing. This was an increase of 2.15% from the original dry weight of the block before it was exposed to the fungi. *R. placenta* however weighed 7.41 kg at the time of test which equates to a 7.72% weight loss. The samples were tested at EMC between 12% and

Table 2. Parameters to be evaluated from ASCE 41-17.

Parameter	Description	Method
F_{max}	Maximum load that the specimen could carry	Maximum on the load deflection curve
Δ_{max}	Displacement at maximum load	Load–deflection curve
ED	Energy dissipated	Area under the curve
D_0	Ductility	The ratio of Δ_{max} to Δ_Y
K_0	Initial slope and slope of the first line in the trilinear model	Slope of initial portion of the backbone curve between 0.1 and 0.4 F_{max}; and ASCE 41-17
K_1	Slope of the second line in the trilinear model	ASCE 41-17
K_2	Slope of the third line in the trilinear model	ASCE 41-17
F_Y	Yield point	5% offset method
Δ_Y	Displacement at yield load	ASCE 41-17
F_U	Ultimate load	Load–deflection curve
Δ_U	Displacement at ultimate load	Load–deflection curve

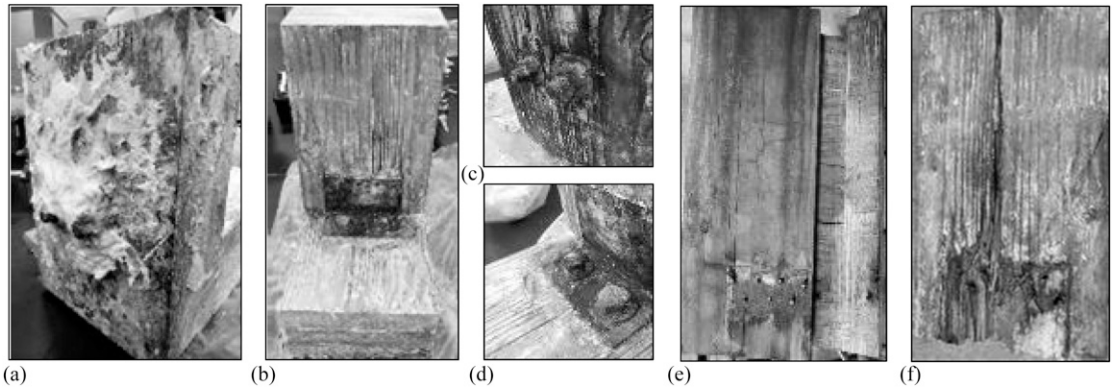

Figure 7. CLT assembly 425 d (14 mo) following exposure to *Rhodonia placenta* using the autoclave bag method: (a) CLT surface with fungal mycelium; (b) fungal mycelium removed; (c and d) steel connection with corrosion; (e and f) connection zones following strength testing.

15%. Curling et al (2001) had reported a daily loss of 0.4% in samples of solid lumber which were infested with brown rot fungi.

Connection Failure

The failure of the connections could be characterized in two ways. As the load was applied, the nail pushed into the wood and the wood fibers gradually broke and gave way. As a result, the nails either pulled out or yielded. The maximum force at which the connections failed varied in the different specimens. A comparison of the backbones of the hysteresis curve from the three specimens (Fig 8) describes the trend. A substantial reduction in capacity, 35% in the tension side and 48% in the compression side, for the specimen infested with *R. placenta* (Fig 8) was observed when compared with the control specimen. In addition, there was a difference in the critical failure mode in each specimen type. Whereas the failure of the wood fibers seems to occur first in the assembly exposed to *R. placenta*, the fibers in the assembly with *G. trabeum* and the control failed late into the test. In the control sample particularly, the authors believe that the cellulose and hemicellulose components of the wooden block were intact, and therefore, the wood fibers possessed adequate strength to resist the cyclic load before ultimately failing.

The average backbone curve of the three specimens was analyzed to characterize the connection strength (Fig 9). A comparison of the three specimens showed a reduction in both tensile and compressive strength as the level of fungal degradation increased. The initial stiffness K_0 calculated using hysteresis backbone generated from the cyclic test protocol was also compared. An initial stiffness of 1056 N/mm was observed in the control specimen. The assembly cultured with *G. trabeum* had an initial stiffness of 1010 N/mm, whereas that exposed to *R. placenta* had an initial stiffness of 788 N/mm.

Table 3. Specimen weight (kg) during 425-d (14-mo) exposure period. Weights during exposure could indicate moisture loss, fungal decomposition of wood, or both.

Fungus	*Rhodonia placenta*	*Gloeophyllum trabeum*
Initial weight	8.03	8.34
Fungal exposure (mo)	10.51 (31% MC)	11.22 (35% MC)
7	9.87	10.6
9	9.07	10.07
14	7.21	8.32

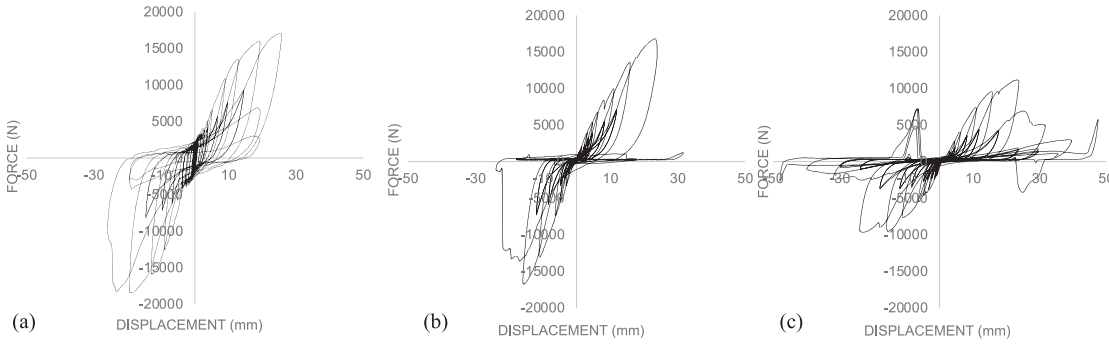

Figure 8. Hysteresis curve: (a) control, (b) *Gloeophyllum trabeum*, (c) *Rhodonia Placenta*.

In addition, the ASCE 41-17 trilinear curve (Fig 10) was developed from the backbone to describe the force–displacement behavior of the connections in the three samples. All the parameters calculated from backbone and the trilinear curves are listed in Table 4. The tensile yield load of the three samples was 10,849N, 7329N, and 7268N respectively (Table 4). The assemblies exposed to *R. placenta* had the lowest yield values and the control being the highest. The maximum load in the three samples was 17,081N, 16,832N, and 11,198N. Again, the control specimen was highest and *R. placenta* infested blocks being the lowest.

The cumulative energy dissipated before the connection failure was computed and is shown in Fig 11. The energy dissipated substantially decreased for *R. placenta* and *G. trabeum* assemblies as shown in Fig 11. Fungal degradation affects the static-tested energy properties, and therefore, the effect of fungal degradation becomes more apparent with regard to the energy dissipated. Although *G. trabeum* assembly did not show much degradation in peak load, the energy dissipated for the same displacement was lower than the control. Similarly, for *R. placenta* assembly, the energy dissipated was substantially lower than that for the control or *G. trabeum* assembly. This closely aligns with Kent et al (2005) that energy dissipation reduces as degradation increases.

CONCLUSIONS AND THE WAY FORWARD

The aim of this study was twofold. First, a method to characterize the effects of biodeterioration on

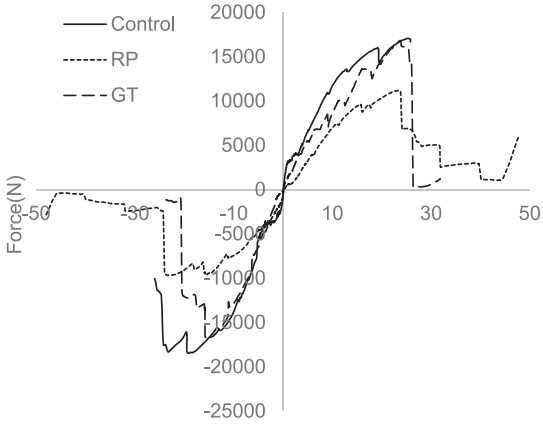

Figure 9. Backbone of the three specimens as obtained from the hysteresis profile.

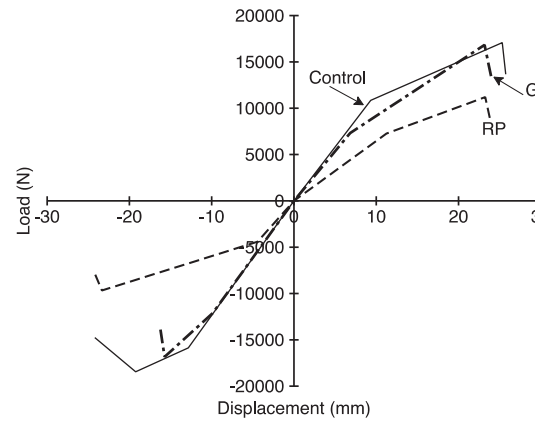

Figure 10. Trilinear idealization as per ASCE 41-17 for the connection performance.

Table 4. Summary of parameters from backbone and ASCE 41-17.

Fungi	Control		*Gloeophyllum trabeum*		*Rhodonia placenta*	
Parameter	Tension	Compression	Tension	Compression	Tension	Compression
F_{max} (N)	17,081	18,448	16,832	16,836	11,198	9675
Δ_{max} (mm)	25.32	19.24	23.16	15.72	23.24	23.34
K_i (N/mm)	1056.4	1144.1	1009.8	1361.6	788.4	950.3
K_0 (N/mm)	1162.8	1236.2	1071.9	1227.1	646.7	994.5
K_1 (N/mm)	389.8	402.5	582.1	806.1	327.4	278.4
K_2 (N/mm)	−8095.2	−743.9	−4272.1	−5805.5	−4028.1	−2126.3
F_Y (N)	10,849	15,872	7329	12,137	7268	4413
Δ_Y (mm)	9.33	12.84	6.84	9.89	11.24	4.44
F_U (N)	13,665	14,758	13,466	13,469	8958	7740
Δ_U (mm)	25.74	24.20	23.95	16.30	23.80	24.25
D_0	2.71	1.50	3.39	1.59	2.07	5.26

the mechanical properties of CLT connections taking fungi which have been established as the most predominant decaying organisms of material as a case study is presented. It represents a preliminary study to work which is already underway at Oregon State University, USA. Two different brown rot fungi were used to conduct this simple study, and only one specimen of each was studied. Two different methods were used to create fungal attack on CLT assemblies. Although they were both successful, one was cumbersome, left room for many errors, and was not as efficient as the other. Second, a procedure and key parameters were introduced to characterize connection performance using the degradation protocol developed.

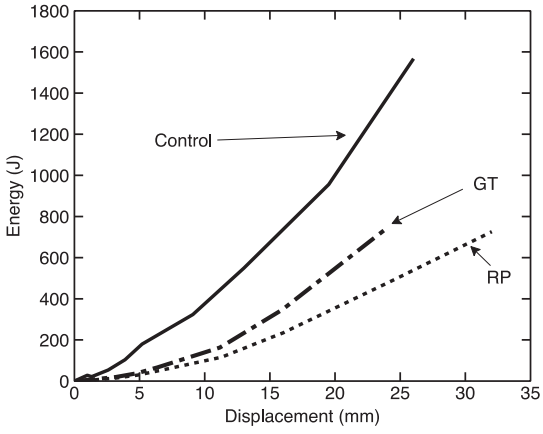

Figure 11. Cumulative energy dissipated with respect to displacement.

The results show that decay fungi will affect the structural assembly, both physically and mechanically. All samples infested showed an unpleasant change in physical properties and a decline in connection strength as the level of fungal infestation increased. The effect of exposure time on the strength CLT was not covered in this study. Experiments are ongoing, and the results will be part of a future publication. The inoculation process and evaluation method developed and presented herein will provide researchers worldwide to conduct biological degradation experiments on MT connections, and the results can be compared across research groups.

ACKNOWLEDGMENTS

The authors would like to extend their deepest gratitude to USDA NIFA AFRI for providing funding for this project (Grant no: 2018-67021-27718). The authors would also like to thank College of Forestry, Oregon State University, for providing funds for the third author to work on the project. The authors would also like to acknowledge the technical help of Milo Clauson and Matt Konkler in the laboratory.

REFERENCES

ASTM (2018) D5764. Test method for evaluating dowel-bearing strength of wood and wood-based products. ASTM. doi: 10.1520/D5764-97AR18.

Barber D (2018) Fire safety of mass timber buildings with CLT in USA. Wood Fiber Sci 50(Special Issue):83-95.

Barbosa AR, Rodrigues L, Sinha A, Higgins C, Zimmerman RB, Breneman S, Pei S, van de Lindt JW, Berman J, McDonnell E, Branco JM, Neves LC (2018) Numerical modelling of CLT diaphragms tested on a shake-table experiment. https://nottingham-repository.worktribe.com/output/1588914/numerical-modelling-of-clt-diaphragms-tested-on-a-shake-table-experiment.

Blomgren H, Pei S, Jin Z, Powers J, Dolan JD, van de Lindt JW, Barbosa AR, Huang D (2019) Full-scale shake table testing of cross-laminated timber rocking shear walls with replaceable components. J Struct Eng 145(10):04019115.

Bolvardi V, Pei S, van de Lindt JW, Dolan JD (2018) Direct displacement design of tall cross laminated timber platform buildings with inter-story isolation. Eng Struct 167: 740-749.

Brandner R, Flatscher G, Ringhofer A, Schickhofer G, Thiel A (2016) Cross laminated timber (CLT): Overview and development. Eur J Wood Wood Prod 74(3):331-351.

Cappellazzi J, Konkler MJ, Sinha A, Morrell JJ (2020) Potential for decay in mass timber elements: A review of the risks and identifying possible solutions. Wood Mater Sci Eng 1-10.

Curling S, Clausen CA, Winandy JE (2001) The effect of hemicellulose degradation on the mechanical properties of wood during brown rot decay. Int Res Group Wood Preserv 2001:1-10.

Fast P, Gafner B, Jackson R, Li J (2016) Case study: An 18 storey tall mass timber hybrid student residence at the University of British Columbia, Vancouver. Page 9 *in* International Holzbau-Forum (IHF) 2016.

Fitzgerald D, Sinha A, Miller TH, Nairn JA (2020) Toe-screwed cross-laminated timber connection design and nonlinear modeling. J Struct Eng 146(6):04020093.

Ganey R, Berman J, Akbas T, Loftus S, Dolan JD, Sause R, Ricles J, Pei S, van de Lindt JW, Blomgren H (2017) Experimental investigation of self-centering cross-laminated timber walls. J Struct Eng 143(10):04017135.

Gaylarde C, Ribas Silva M, Warscheid Th (2003) Microbial impact on building materials: An overview. Mater Struct 36(5):342-352.

Glass SV, Wang J, Easley S, Finch G (2013) Chapter 10: Enclosure–Building enclosure design for cross-laminated timber construction. Pages 1-55 *in* E Karacabeyli and B Douglas, eds. CLT handbook: Cross-laminated timber, Vol. 10 (Special Publication, ISSN 1925-0495; SP-529E). https://www.fs.usda.gov/treesearch/pubs/all/43846.

Hasburgh L, Bourne K, Ranger L, Dagenais C, Roy-Poirier A (2016a) Fire performance of mass-timber encapsulation methods and the effect of encapsulation on char rate of cross-laminated timber. Page 10 *in* World Conference on Timber Engineering, August 22-25, 2016, Vienna, Austria.

Hasburgh L, Schiff S, Pang W, Peralta P, Mitchell P, Bourne K (2016b) Effect of adhesives and ply configuration on the fire performance of southern pine cross-laminated timber. Page 10 *in* World Conference on Timber Engineering, August 22-25, 2016, Vienna, Austria.

Kent SM, Leichti RJ, Rosowsky DV, Morrell JJ (2005) Effects of decay on the cyclic properties of nailed connections. J Mater Civ Eng 17(5):579-585.

Kent SM, Leichti RJ, Rosowsky DV, Morrell JJ (2007) Effects of wood decay by *Postia placenta* on the lateral capacity of nailed oriented strandboard sheathing and Douglas-fir framing members. Wood Fiber Sci 36(4): 560-572.

Kippel M, Leyder C, Frangi A, Fontana M (2014) Fire tests on loaded cross-laminated timber wall and floor elements. Fire Saf Sci 11:626-639.

Kramer A, Barbosa AR, Sinha A (2014) Viability of hybrid poplar in ANSI approved cross-laminated timber applications. J Mater Civ Eng 26(7):06014009.

Kramer A, Barbosa AR, Sinha A (2016) Performance of steel energy dissipators connected to cross-laminated timber wall panels subjected to tension and cyclic loading. J Struct Eng 142(4):E4015013.

Krawinkler H, Parisi F, Ibarra L, Ayoub A, Medina R (2001) Development of a testing protocol for woodframe structures. 99 pp.

Kremer PD, Symmons MA (2015) Mass timber construction as an alternative to concrete and steel in the Australia building industry: A PESTEL evaluation of the potential. Int Wood Prod J 6(3):138-147.

Mahdavifar V, Barbosa AR, Sinha A, Muszynski L, Gupta R (2017) Hysteretic behaviour of metal connectors for hybrid (high- and low-grade mixed species) cross laminated timber. ArXiv:1710.07825 [Physics]. http://arxiv.org/abs/1710.07825.

Mahdavifar V, Barbosa AR, Sinha A, Muszynski L, Gupta R, Pryor SE (2019) Hysteretic response of metal connections on hybrid cross-laminated timber panels. J Struct Eng 145(1):04018237.

Mahr K, Sinha A, Barbosa AR (2020) Experimental investigation and modeling of thermal effects on a typical cross-laminated timber bracket shear connection. J Mater Civ Eng 32(6):04020111.

Mallo MFL, Espinoza O (2014) Outlook for cross-laminated timber in the United States. BioResources 9(4):7427-7443.

Mankowski M, Morrell JJ (2000) Patterns of fungal attack in wood-plastic composites following exposure in a soil block test. Wood Fiber Sci 32(3):340-345.

Miyamoto BT, Sinha A, Morrell I (2020) Connection performance of mass plywood panels. For Prod J 70(1):88-99.

Morrell JJ, Morrell I, Sinha A, Trebelhorn D (2018) Moisture intrusion in cross laminated timber and the potential for fungal attack. World Conference on Timber Engineering, August 20-23, 2018, Seoul, South Korea.

Pei S, van de Lindt JW, Barbosa AR, Berman JW, McDonnell E, Dolan JD, Blomgren H, Zimmerman RB, Huang D, Wichman S (2019) Experimental seismic response of a resilient 2-story mass-timber building with post-tensioned rocking walls. J Struct Eng 145(11):04019120.

Pei S, van de Lindt JW, Popovski M, Berman JW, Dolan JD, Ricles J, Sause R, Blomgren H, Rammer DR (2016) Cross-laminated timber for seismic regions: Progress and

challenges for research and implementation. J Struct Eng 142(4):E2514001.

Schmidt T, Blass HJ (2018) Recent development in CLT connections: Part II plane shear connections for CLT bracing elements under cycling loads. Wood Fiber Sci 50(Special Issue):58-67.

Schmidt EL, Riggio M, Barbosa AR, Mugabo I (2019) Environmental response of a CLT floor panel: Lessons for moisture management and monitoring of mass timber buildings. Build Environ 148:609-622.

Soti R, Sinha A, Morrell I, Miyamoto BT (2020) Response of self-centering mass plywood panel shear walls. Wood Fiber Sci 52(1):102-116.

Tannert T, Follesa M, Fragiacomo M, Gonzalez P, Isoda H, Moroder H, Xiong H, van de Lindt JW (2018) Seismic design of cross-laminated timber buildings. Wood Fiber Sci 50(special issue):3-26.

Tugce A, Sause R, Ricles J, Ganey R, Berman J, Loftus S, Dolan JD, Pei S, van de Lindt JW, Blomgren H (2017) Analytical and experimental lateral-load response of self-centering posttensioned CLT walls. J Struct Eng 143(6): 04017019.

van de Lindt JW, Furley J, Amini MO, Pei S, Tamagnone G, Barbosa AR, Rammer D, Line P, Fragiacomo M, Popovski M (2019) Experimental seismic behavior of a two-story CLT platform building. Eng Struct 183:408-422.

Wang JY, Stirling R, Morris PI, Taylor A, Lloyd J, Kirker G, Lebow S, Mankowski M, Barnes HM, Morrell JJ (2018) Durability of mass timber structures: A review of the biological risks. Wood Fiber Sci 50(Special Issue): 110-127.